Chaos, Solitons and Fractals 154 (2022) 111700

Contents lists available at ScienceDirect

Chaos, Solitons and Fractals

Nonlinear Science, and Nonequilibrium and Complex Phenomena

journal homepage: www.elsevier.com/locate/chaos

Deep learning systems for automatic diagnosis of infant cry signals

Salim Lahmiri[a,b,*], Chakib Tadj[b], Christian Gargour[b], Stelios Bekiros[c,d,e]

[a] Department of Supply Chain and Business Technology Management, John Molson School of Business, Concordia University, Montreal, Canada
[b] Department of Electrical Engineering, École de Technologie Supérieure, Montreal, Canada
[c] European University Institute, Florence, Italy
[d] Wilfrid Laurier University, Waterloo, Canada
[e] IPAG Business School, Department of Finance and Information Systems, Paris, France

ARTICLE INFO

Article history:
Received 12 November 2021
Accepted 1 December 2021

Keywords:
Deep learning
Deep feedforward neural networks
Long short-term memory neural networks
Convolutional neural networks
Infant cry record
Classification

ABSTRACT

Nowadays, deep learning architectures are promising artificial intelligence systems in various applications of biomedical engineering. For instance, they can be combined with signal processing techniques to build computer-aided diagnosis systems used to help physician making appropriate decision related to the diagnosis task. The goal of the current study is to design and validate various deep learning systems to improve diagnosis of infant cry records. Specifically, deep feedforward neural networks (DFFNN), long short-term memory (LSTM) neural networks, and convolutional neural networks (CNN) are designed, implemented and trained with cepstrum analysis-based coefficients as inputs to distinguish between healthy and unhealthy infant cry records. All deep learning systems are validated on expiration and inspiration sets separately. The number of convolutional layers and number of neurons in hidden layers are respectively varied in CNN and DFFNN. It is found that CNN achieved the highest accuracy and sensitivity, followed by DFFNN. The latter, obtained the highest specificity. Compared to similar work in the literature, it is concluded that deep learning systems trained with cepstrum analysis-based coefficients are powerful machines that can be employed for accurate diagnosis of infant cry records so as to distinguish between healthy and pathological signals.

1. Introduction

Very recently, deep learning neural networks have been applied to various biomedical engineering problems; including classifications of day 3 human embryo [1], osteosarcoma recognition in histological images [2], breast mass and tumor diagnosis [3,4], pulmonary coccidioidomycosis detection [5], blood pressure measurement [6], EEG classification [7], skin cancer diagnosis [8], clinical depression assessment [9], COVID-19 detection [10,11], drug-target interactions prediction [12], brain magnetic resonance image analysis [13,14], segmentation of deep foveal avascular zone [15], Parkinson speech recognition [16], and hemorrhage detection in retina [17]. Thanks to deep neural network architectures with multiple layers and neurons, such systems were found to be effective in performing high-complexity tasks in biomedical engineering [1–17].

Besides, infant cry record analysis for medical diagnosis in clinical milieu is receiving a growing attention as a non-invasive technique. Indeed, various machine learning methods have been employed to distinguish between healthy and unhealthy infant cry records; namely, hidden Markov models [18], probabilistic neural network [19], and linear support vector machines [20], and deep feedforward neural networks [21]. The Hidden Markov Models trained with segmented cry signals achieved 83.79% accuracy [18], the probabilistic neural network trained with prevalence of fundamental frequency glide, resonance frequencies dysregulation, and Mel-frequency cestrum coefficients yielded to an accuracy varying from 67.00% to 88.71% [19], the linear SVM trained with Mel-frequency cepstral coefficients, tilt, and rhythm features obtained 67.80% accuracy [20], and deep feedforward neural networks achieved 100% accuracy [21].

To extend the literature on infant cry record classification and on applications of deep learning in biomedical engineering problems, the goal of our work is to examine the effectiveness of various deep learning neural networks when used in the diagnosis of infant cry records. Specifically, we focus exclusively on three different deep learning systems and compare their respective performances. Indeed, we focus on deep learning systems as they were found to be useful in various biomedical engineering applications [1–17].

To sum up, the chosen deep learning neural networks to distinguish between healthy and unhealthy infant cries are deep feedforward neural networks (DFFNN), long short-term memory (LSTM)

* Corresponding author.
E-mail address: salim.lahmiri@concordia.ca (S. Lahmiri).

https://doi.org/10.1016/j.chaos.2021.111700
0960-0779/

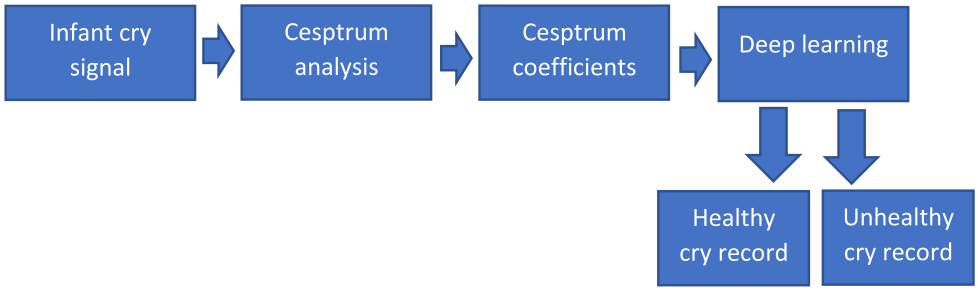

Fig. 1. Flowchart of a computer model for diagnosis of infant cry record based on cepstrum analysis and classification by deep learning systems.

neural networks, and convolutional neural networks (CNN). The inputs to each deep learning system are cepstrum based coefficients obtained from the original cry signals. Indeed, we choose them to train deep learning systems as they were found to be statistically significant in differentiating between healthy and unhealthy infant cry records [22]. In this regard, the contributions of our paper can be summarized as follows:

i We pioneer the evaluation of the performance of various deep learning systems in the task of infant cry record classification to distinguish between healthy and unhealthy infants. Specifically, deep feedforward neural networks (DFFNN), long short-term memory (LSTM) neural networks, and convolutional neural networks (CNN) are evaluated and compared.
ii Various topologies of CNN and various number of hidden neurons in DFFNN are examined since the performances of these networks depend on such factors.
iii We extend our previous work [22] by using cepstrum based-coefficients as inputs to deep learning architectures.
iv Our study enriches the literature on infant cry record classification for medical diagnosis purpose by applying, evaluating and comparing deep learning techniques.

The rest of the paper is organized as follows. Section 2 introduces cepstrum analysis, DFFNN, LSTM, and CNN. Section 3 presents data and experimental results. Finally, Section 3 concludes the study.

2. Methods

In the current study, three deep learning neural networks are implemented to classify healthy and unhealthy infant cries; namely, DFFNN, LSTM, and CNN. They are all trained with cepstrum based-coefficients as inputs. The performance of each deep learning system is evaluated by using standard machine learning performance techniques including accuracy, sensitivity, and specificity. Fig. 1 shows flowchart of the automated system for infant cry signal analysis and classification.

All methods are presented next.

2.1. Cepstral analysis

Cepstrum analysis [23] is suitable to describe harmonics in signals. In this regard it was largely applied in biomedical engineering problems including epileptic seizure detection [24], assessing Parkinson's disease severity [25], classification of heart sounds [26], and estimation of heartbeat rate [27], and newborn cry diagnostic [22]. In our study, we make use of cepstrum analysis to describe harmonics in infant cry records.

Technically speaking, the cepstrum $C[n]$ is computed as the inverse discrete Fourier transform (IDFT) of the log magnitude of the DFT of a signal $x[n]$, which is given as follows:

$$C[n] = IDFT\{\log|DFT(x[n])|\} \quad (1)$$

In general, the number of coefficients used to describe the cepstrum can be set arbitrarily. In our work, it is fixed to one thousand to obtain good representation of cry record harmonics and to make convergence of each deep neural network system fast.

2.2. DFNN

The deep feed-forward neural networks (DFFNN) are basically feed-forward neural networks with multiple hidden layers. In this regard, the DFFNN can learn to transform from one-level description into a multi-level one to deal with complex and high nonlinear problems. Recently, the DFFNN have been successfully applied in detection of sepsis [28], prediction of post-liver transplant mortality [29], and type 2 diabetes patient diagnosis [30].

Recall that each layer in DFFNN utilizes a nonlinear transformation on its input and provides a representation in its output. By assuming that the DFFNN architecture is composed of N layers and each layer has j units (neurones), the output signal of the $(l)^{th}$ layer (l = 1,2,3,...,N) is given by:

$$z_j^l = f\left(w_j^T a_j^{l-1} + b_j\right) \quad (2)$$

where f is the activation function, w is the weight vector, a is the output signal in a particular layer, and b is the bias parameter.

In this study, the sigmoid function is chosen to be the activation function and the resilient backpropagation algorithm is chosen to train the network to avoid limits of the standard steepest descent algorithm. For the experiments, the input layer has 1000 neurones corresponding to samples of the cepstrum and we will try multiple hidden layers (from 1 to 3) and multiple number of neurones in each layer: 250, 500, and 750.

2.3. LSTM

The long-short term memory (LSTM) networks [31] are robust to vanishing gradient problem that can be encountered by RNN. To overcome such limit, the LSTM incorporates memory cells to replace traditional nodes of recurrent neural networks (RNN). Their major role is to store information for learning. Hence, the long sequence learning process is improved under LSTM. The LSTM networks were found to be effective in various biomedical engineering applications including identification of autism disorder [32], sensory processing [33], and analysis of EEG for visual object classification [34].

The memory cell contains four parts; namely, cell state (c), forget gate (f), input gate (i), and output gate (o). They mathematically expressed as follows:

$$f_t = S\left(\omega_f[x_t, h_{t-1}] + b_f\right) \quad (3)$$

$$i_t = S(\omega_i[x_t, h_{t-1}] + b_i) \quad (4)$$

$$o_t = S(\omega_0[x_t, h_{t-1}] + b_0) \quad (5)$$

$$c_t = f_t \cdot c_{t-1} + i_t \cdot tanh(\omega_c[x_t, h_{t-1}] + b_c) \quad (6)$$

$$h_t = o_t \cdot tanh(c_t) \quad (7)$$

where x_t is the input state, h_t is the hidden state, c_t is the memory cell state; and, ω and b are their respective weight matrices and bias vectors. Here, S is the softmax function used to calculate the highest probability to perform classification. Recall that the cell state c_t and the output htrepresent short-term memory and long-term memory respectively. In this work, the LSTM has two fully connected layers, number of epochs is set to 50, and the adaptive moment estimation method is employed since it is suitable to train LSTM systems.

2.4. CNN

The convolutional neural networks (CNN) are common deep feed-forward artificial neural networks originally introduced by LeCun et al., [35]. It is suitable for deep features extraction as its topology makes it invariant to translation and rotation in inputs. In addition, compared common deep feed-forward artificial neural networks, CNN require less parameters to be tuned. Examples of successful applications of CNN include analysis of surface electromyography for hand prosthetics [36], lung sound diagnosis [37], breast ultrasonography images [38], and hemorrhage detection in retina [17].

The general topology of CNN consists of one or more hidden convolutional layers and a fully connected layer at the top, including associated weights and pooling layers. In the convolutional layer, a convolution of each subregion of the input data with a kernel is calculated. Then, the convolution output result is added to a bias and processed by an activation function to generate a feature map for the next layer. For instance, If the cepstrum input vector is $x_i^0 = [x_1, x_2, \ldots, x_n]$ where n is the number of samples in cepstrum, then output values are calculated as follows:

$$c_i^{l,j} = h\left(b_j + \sum_{m=1}^{M} w_m^j x_{i+m-1}^{oj}\right) \quad (8)$$

where l is the layer index, h is a nonlinear activation function, b is bias term associated with the jth feature map, M is the kernel (filter) size, and w is the weight.

The pooling layer is subsequent to the convolutional layer and used to apply a down-sampling operation to features vector so as to reduce its size. In our study, the max-pooling operation is adopted to compute the maximum value in a set of nearby inputs. Hence, the pooling of a feature map in a layer is expressed as follows:

$$p_i^{l,j} = \max_{r \in R} c_{i \times T + r}^{l,j} \quad (9)$$

where R and T are respectively the size of the pooling window and the pooling stride. Recall that several pooling layers are inserted between successive convolutional layers to finally obtain deep features used for classification purpose. Finally, the classification layer is a fully connected layer used to perform the high-level reasoning about the deep features and produce the classification output. In our experiments, the stochastic gradient descent with momentum (SGDM) algorithm is adopted to train CNN, the number of epochs is set to 50, and the number of convolutional layers varies from one to three.

2.5. Performance measures and protocol of experiments

We evaluate the performance of the classification deep learning systems by using accuracy (correct classification rate), sensitivity, and specificity. They are calculated as follows:

$$Accuracy = \frac{TN + TP}{TN + FN + TP + FP} \quad (10)$$

$$Sensitivity = \frac{TP}{TP + FN} \quad (11)$$

$$Specificity = \frac{TN}{TN + FP} \quad (12)$$

where TN is number of true negatives, TP is number of true positives, FN is number of false negatives, and FP is number of false positives. In this study, the positive and negative cases were assigned to unhealthy and healthy cry signals. For robustness of the experimental results, 10-fold cross-validation protocol is adopted. The 10-fold validation is commonly employed in machine learning literature. The dataset is divided into 10 folds and each fold has the chance to be tested, such that all folds are used for training and testing. Accordingly, the mean and standard deviation of each performance metric are calculated.

3. Data and results

We used our database in [21,22] to describe the comparative study of DFFNN, LSTM, and CNN in distinguishing between healthy and unhealthy infant cry signals. Cry signals were recorded in Sainte-Justine hospital (Montreal, Canada), Al-Sahel hospital (Lebanon) and Al-Raee hospital (Lebanon). The database is composed of expiration (EXP) set with 2638 cry signals (1319 healthy signals and 1319 unhealthy signals) and inspiration set (INS) with 1860 cry signals (930 healthy signals and 930 unhealthy signals).

The database contains cry records from male and female babies and their ages vary from one to fifty-three days. Unhealthy babies are affected with various disorders; for instance, those related to central nervous system, respiratory system, blood, pediatric chromosomal anomaly, and congenital cardiac malformations.

All signals were recorded by using a two-channel sound recorder with a sampling frequency of 44.1 kHz at 16 bits and 10 cm to 30 cm from the baby. The length of each signal is from two to three minutes. Background noise and artifacts are filtered out from each signal. Also, Wave Surfer tool was employed to segment each record so as to save only respiration and expiration episodes. Fig. 2 shows examples of healthy (normal) and unhealthy (abnormal) cry records and Fig. 3 plots examples of cepstrums representing healthy and unhealthy cry records.

After cepstrum coefficients used to form features of all samples are obtained, the constructed deep learning systems can be employed to distinguish between healthy and unhealthy infant cry signals. For statistical robustness of the experimental results, the dataset is divided into ten folds to perform cross-validation method. Specifically, the training and testing phases are carried out by using nine folds for training and the rest is utilized for validation. This protocol is repeated ten times to assure that all folds are used for training and for testing as well. Finally, the average values and standard deviations of accuracy, sensitivity, and specificity are computed for each single deep learning system. In our experiments, cepstral analysis and deep learning systems were implemented in Matlab©R2021b environment. The obtained performance metrics are provided in Table 1.

Accordingly, CNN with 1 convolutional layer yielded to the highest accuracy on expiration set (95.31%±0.0320) followed by CNN with 2 convolutional layers (95.28%±0.0222), and CNN with 3 convolutional layers (94.33%±0.0272). The DFFNN with 750 hidden neurons achieved the lowest accuracy (80.00%±0.0000) on expiration set. Hence, CNN outperformed LSTM and DFFNN on expiration in terms of correct classification rate (accuracy). Besides, LSTM achieved the lowest accuracy (83.89%±0.1410). Also,

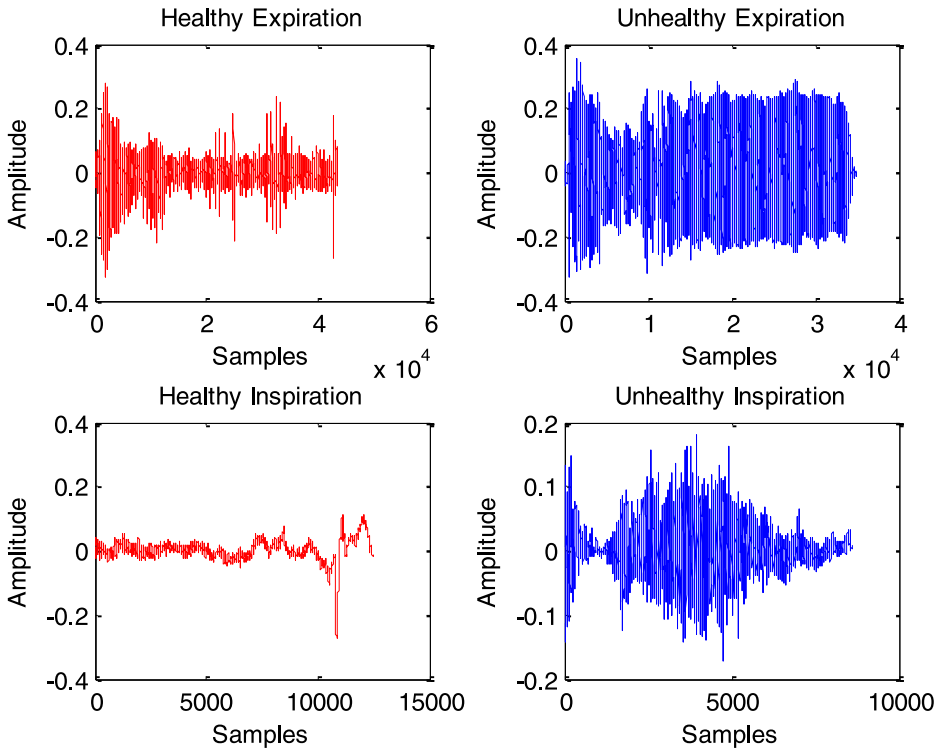

Fig. 2. Plots of normal and abnormal infant cry signals.

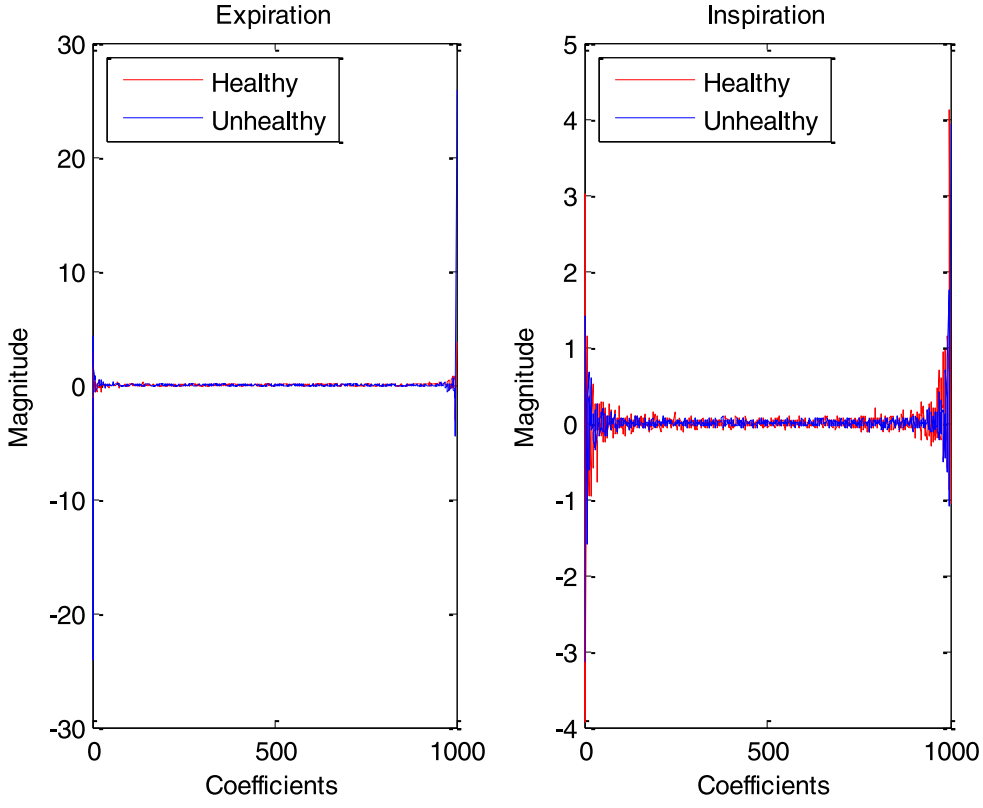

Fig. 3. Plots of cepstrums from normal and abnormal infant cry signals.

Table 1
Performance measures obtained by using 10-fold cross-validation protocol.

	Accuracy	Sensitivity	Specificity
Expiration set			
CNN with 1 Convolutional layer	95.31%±0.0320	95.42%±0.0838	95.21%±0.1333
CNN with 2 Convolutional layers	95.28%±0.0222	99.30%±0.0813	91.26%±0.0930
CNN with 3 Convolutional layers	94.33%±0.0272	94.82%±0.1610	93.81%±0.1724
LSTM	83.89%±0.1410	89.83%±0.4254	77.98%±0.3977
DFFNN with 250 hidden neurons	80.23%±0.0000	30.88%±0.0029	99.58%±0.0029
DFFNN with 500 hidden neurons	79.70%±0.0000	98.85%±0.0000	50.55%±0.0000
DFFNN with 750 hidden neurons	80.00%±0.0000	98.48%±0.0000	31.52%±0.0000
Inspiration set			
CNN with 1 Convolutional layer	86.83%±0.0280	82.58%±0.1792	91.08%±0.1798
CNN with 2 Convolutional layers	92.04%±0.0433	91.40%±0.1384	92.69%±0.1211
CNN with 3 Convolutional layers	90.05%±0.0269	92.47%±0.1032	87.63%±0.0962
LSTM	80.18%±0.0051	90.32%±0.4779	60.00%±0.4830
DFFNN with 250 hidden neurons	80.05%±0.0000	99.14%±0.0000	50.97%±0.0000
DFFNN with 500 hidden neurons	80.01%±0.0000	30.89%±0.0000	99.12%±0.0000
DFFNN with 750 hidden neurons	79.84%±0.0000	30.75%±0.0282	98.92%±0.0279

CNN with 2 Convolutional layers yielded to the highest sensitivity (99.30%±0.0813) followed by DFFNN with 500 hidden neurons (98.85%±0.0000), and LSTM obtained 89.83%±0.4254. In terms of sensitivity performance, DFFNN with 250 hidden neurons obtained the highest value (99.58%±0.0029) followed by CNN with 1 convolutional layer (95.21%±0.1333), and LSTM yielded to 89.83%±0.4254. In short, on expiration set, CNN outperformed DFFNN and LSTM in terms of accuracy and sensitivity, while DFFNN outperformed CNN and LSTM in terms of specificity as indicated in Table 1.

Experimental results from inspiration set provided in Table 1 indicate that CNN with 2 convolutional layers achieved the highest accuracy (92.04%±0.0433), LSTM obtained 80.18%±0.0051, and DFFNN with 750 hidden neurons yielded to the lowest accuracy (79.84%±0.0000). Besides, DFFNN with 250 hidden neurons obtained the highest sensitivity (99.14%±0.0000) and DFFNN with 750 hidden neurons obtained the lowest sensitivity (30.75%±0.0282). Finally, DFFNN with 500 hidden neurons yielded to the highest specificity (99.12%±0.0000) followed by CNN with 2 convolutional layers (92.69%±0.1211), LSTM achieved 60.00%±0.4830, and DFFNN with 250 hidden neurons obtained the lowest specificity (50.97%±0.0000). In short, on inspiration set, CNN obtained the highest accuracy while DFFNN achieved the highest sensitivity and specificity.

To summarize, CNN outperformed both LSTM and DFFNN in terms of accuracy on both expiration and inspiration sets. Its best accuracy is obtained on expiration set. Also, its accuracy performance slightly decreases with number of convolutional layers.

To complete the 10-fold cross-validation on expiration set, the DFFNN took respectively 23.24 s, 9.02 s, and 15.73 s to run with 250, 500, and 750 neurons in each hidden layer. The LSTM took 60.32 s and CNN took 208.30 s, 446.72 s, and 536.03 to run with one, two, and three convolutional layers respectively. Besides, to complete the 10-fold cross-validation on inspiration set, the DFFNN took respectively 4.03 s, 24.62 s, and 11.17 s to run with 250, 500, and 750 neurons in each hidden layer. The LSTM took 50.22 s and CNN took 181.36 s, 270.72 s, and 342.39 s respectively to run with one, two, and three convolutional layers. In this regard, the DFFNN is faster in training and testing compared to CNN and LSTM. This can be attributed to the resilient backpropagation algorithm used to train the DFFNN.

Recall that the best deep neural network is CNN with one convolutional layer as it achieved 95.31%±0.0320 accuracy, 95.42%±0.0838 sensitivity, and 95.21%±0.1333 specificity. In this regard, CNN trained with cepstrum coefficients outperformed similar models applied to the same problem; including the Hidden Markov Models trained with segmented cry signals (83.79% accuracy) [18], the probabilistic neural network trained with prevalence of fundamental frequency glide, resonance frequencies dysregulation, and Mel-frequency cestrum coefficients (67.00% to 88.71% accuracy) [19], the linear SVM trained with Mel-frequency cepstral coefficients, tilt, and rhythm features (67.80% accuracy) [20]. However, it underperformed deep feedforward neural networks trained with cepstrum coefficients where 100% accuracy was obtained [21]. Bring in mind that the work in [21] used the same number of neurons in each hidden number as the number of neurons in the input layer. This could improve the learning ability of the network.

The obtained experimental results suggest that deep learning architectures trained with cepstrum coefficients yield to better accuracy in terms of distinguishing between healthy and unhealthy infant cry records as opposed to existing works found in the literature) [18–20]. This can be explained by the statistical significance of cepstrum coefficients to characterize infant normal and abnormal cry signals) [22] and the powerful learning ability of deep learning systems. Hence, such computer-aided diagnosis systems are promising in clinical milieu.

4. Conclusion

Deep learning systems are making major advances in the design of computer-aided diagnosis systems for healthcare. The aim of our paper is to compare the performance of three different deep learning systems in the task of distinguishing between recorded healthy and pathological infant cry signals. In this regard, cepstrum analysis is employed to describe harmonics in expiration and inspiration cry record and the resulting spectrum is fed to DFFNN, LSTM, and CNN.

Experimental results from expiration and inspiration sets indicated that CNN outperformed DFNN and LSTM in terms of accuracy and sensitivity, whilst DFNN yielded to the highest. In comparison with similar studies, our findings suggest that deep learning systems trained with cepstrum descriptors obtained the highest accuracy; hence, they are promising for analysis and diagnosis of infant cry signals in clinical milieu.

Declaration of Competing Interest

The authors declare that they have no known competing financial interests or personal relationships that could have appeared to influence the work reported in this paper.

Acknowledgment

This research is partly supported by the Natural Sciences and Engineering Research Council of Canada (NSERC) [RGPIN-2016-05067].

References

[1] Wu C, Yan W, Li H, Li J, Wang H, Chang S, et al. A classification system of day 3 human embryos using deep learning. Biomed Signal Process Control 2021;70:102943.
[2] Anisuzzaman DM, Barzekar H, Tong L, Luo J, Yu Z. A deep learning study on osteosarcoma detection from histological images. Biomed Signal Process Control 2021;69:102931.
[3] Byra M. Breast mass classification with transfer learning based on scaling of deep representations. Biomed Signal Process Control 2021;69:102828.
[4] Zhang Z, Li Y, Wu W, Chen H, Cheng L, Wang S. Tumor detection using deep learning method in automated breast ultrasound. Biomed Signal Process Control 2021;68:102677.
[5] Ott J, Bruyette D, Arbuckle C, Balsz D, Hecht S, Shubitz L, et al. Detecting pulmonary Coccidioidomycosis with deep convolutional neural Networks. Mach Learn Appl 2021;5:100040.
[6] Pan F, He P, Wang H, Xu Y, Pu X, Zhao Q, et al. Development and validation of a deep learning-based automatic auscultatory blood pressure measurement method. Biomed Signal Process Control 2021;68:102742.
[7] Li M, Chen W. FFT-based deep feature learning method for EEG classification. Biomed Signal Process Control 2021;66:102492.
[8] Ali MS, Miah MS, Haque J, Rahman MM, Islam MK. An enhanced technique of skin cancer classification using deep convolutional neural network with transfer learning models. Mach Learn Appl 2021;5:100036.
[9] Muzammel M, Salam H, Hoffmann Y, Chetouani M, Othmani A. AudVowelConsNet: a phoneme-level based deep CNN architecture for clinical depression diagnosis. Mach Learn Appl 2020;2:100005.
[10] JavadiMoghaddam S, Gholamalinejad H. A novel deep learning based method for COVID-19 detection from CT image. Biomed Signal Process Control 2021;70:102987.
[11] Nigam B, Nigam A, Jain R, Dodia S, Arora N, Annappa B. COVID-19: automatic detection from X-ray images by utilizing deep learning methods. Expert Syst Appl 2021;176:114883.
[12] Mahdaddi A, Meshoul S, Belguidoum M. EA-based hyperparameter optimization of hybrid deep learning models for effective drug-target interactions prediction. Expert Syst Appl 2021;185:115525.
[13] Rai HM, Chatterjee K. Detection of brain abnormality by a novel Lu-Net deep neural CNN model from MR images. Mach Learn Appl 2020;2:100004.
[14] Karayegen G, Aksahin MF. Brain tumor prediction on MR images with semantic segmentation by using deep learning network and 3D imaging of tumor region. Biomed Signal Process Control 2021;66:102458.
[15] Guo M, Zhao M, Cheong AM, Corvi F, Chen X, Chen S, et al. Can deep learning improve the automatic segmentation of deep foveal avascular zone in optical coherence tomography angiography? Biomed Signal Process Control 2021;66:102456.
[16] Ma J, Zhang Y, Li Y, Zhou L, Qin L, Zeng Y, et al. Deep dual-side learning ensemble model for Parkinson speech recognition. Biomed Signal Process Control 2021;69:102849.
[17] Lahmiri S. Hybrid deep learning convolutional neural networks and optimal nonlinear support vector machine to detect presence of hemorrhage in retina. Biomed Signal Process Control 2020;60:101978.
[18] Abou-Abbas L, Fersaie Alaie H, Tadj C. Automatic detection of the expiratory and inspiratory phases in newborn cry signals. Biomed Signal Process Control 2015;19:35–43.
[19] Kheddache Y, Tadj C. Identification of diseases in newborns using advanced acoustic features of cry signals. Biomed Signal Process Control 2019;50:35–44.
[20] Salehian Matikolaie F, Tadj C. On the use of long-term features in a newborn cry diagnostic system. Biomed Signal Process Control 2020;59:101889.
[21] Lahmiri S, Tadj C, Gargour C. Biomedical Diagnosis of infant cry signal based on analysis of cepstrum by deep feedforward artificial neural networks. IEEE Instrum Meas Mag 2020;24:24–9.
[22] Lahmiri S, Tadj C, Gargour C, Bekiros S. Characterization of infant healthy and pathological cry signals in cepstrum domain based on approximate entropy and correlation dimension. Chaos, Solitons Fractals 2021;143:110639.
[23] Childers DG, Skinner DP, Kemerait RC. The Cepstrum: a Guide to Processing. Proc IEEE 1977;65:1428–43.
[24] Yavuz E, Kasapbaşi MC, Eyüpoğlu C, Yazıcı R. An epileptic seizure detection system based on cepstral analysis and generalized regression neural network. Biocybern Biomed Eng 2018;38:201–16.
[25] Khan T, Lundgren LE, Anderson DG, Nowak I, Dougherty M, Verikas A, et al. Assessing Parkinson's disease severity using speech analysis in non-native speakers. Comput Speech Lang 2020;61 Article 101047.
[26] Abduh Z, Nehary EA, Abdel Wahed M, Kadah YM. Classification of heart sounds using fractional Fourier transform based mel-frequency spectral coefficients and traditional classifiers. Biomed Signal Process Control 2020;57 Article 101788.
[27] Ankıshan H. Estimation of heartbeat rate from speech recording with hybrid feature vector (HFV). Biomed Signal Process Control 2019;49:483–92.
[28] Kam HJ, Kim HY. Learning representations for the early detection of sepsis with deep neural networks. Comput. Biol. Med. 2017;89:248–55.
[29] Ershoff BD, Lee CK, Wray CL, Agopian VG, Urban G, Baldi P, et al. Training and validation of deep neural networks for the prediction of 90-day post-liver transplant mortality using UNOS registry data. Transplant. Proc. 2020;52:246e258.
[30] Kannadasan K, Edla DR, Kuppili V. Type 2 diabetes data classification using stacked autoencoders in deep neural networks. Clin Epidemiol Glob Health 2019;7:530–5.
[31] Hochreiter S, Schmidhuber J. Long short-term memory. Neural Comput 1997;9:1735–80.
[32] Xu L, Sun Z, Xie J, Yu J, Li J, Wang J. Identification of autism spectrum disorder based on short-term spontaneous hemodynamic fluctuations using deep learning in a multi-layer neural network. Clin Neurophysiol 2021;132:457–68.
[33] Pinotsis DA, Siegel M, Miller EK. Sensory processing and categorization in cortical and deep neural networks. Neuroimage 2019;202:116118.
[34] Zheng X, Chen W. An Attention-based Bi-LSTM Method for Visual Object Classification via EEG. Biomed Signal Process Control 2021;63:102174.
[35] LeCun Y, Boser B, Denker JS, Henderson D, Howard RE, Hubbard W, et al. Backpropagation applied to handwritten zip code recognition. Neural Comput 1989;1:541–51.
[36] Atzori M, Cognolato M, Müller H. Deep learning with convolutional neural networks applied to electromyography data: a resource for the classification of movements for prosthetic hands. Front Neurorobot 2016;10 Article 9.
[37] Messner E, Fediuk M, Swatek P, Scheidl S, Smolle-Jüttner F-M, Olschewski H, et al. Multi-channel lung sound classification with convolutional recurrent neural Networks. Comput. Biol. Med. 2020;122:103831.
[38] Qi X, Zhang L, Chen Y, Pi Y, Chen Y, Lv Q, et al. Automated diagnosis of breast ultrasonography images using deep neural networks. Med Image Anal 2019;52:185–98.